ARCHIVES OF ACOUSTICS
16, 1, 149-156(1991)

$LINbO_3$ DISPERSIVE FILTER WITH FAN-SHAPED TRANSDUCERS AND REFLECTIVE ARRAYS

P. V. VIKTOROV, A. R. ZHEZHERIN, L. P. KONOVALOVA

Leningrad Institute of Aviation Instrument Making
(190 000, Leningrad, USSR)

At present, dispersive devices with reflective arrays (RAC) are used for radiosignal processing. RAC with unidistant transducers and U-path of acoustic waves with dispersive slanted transducers and slanted reflective arrays (RA) described in literature, have rather high interreflections in RA. This affects the pulse of a device.

In the presented work, RAC with fan-shaped transducers (FST) and slanted RA is described. An analysis of the amplitude distribution of the FST acoustic field and the dependence of the maximum of the distribution in FST aperture on instantaneous frequency are presented. Basing on this analysis and the type of the dispersive characteristic of a device, the relations for RA parameters are obtained. The parameters of the prototypes fabricated of the YZ-$LiNbO_3$ piezosubstrate are presented. An analysis of the results obtained is performed.

1. Introduction

At present, dispersive SAW filters with reflective arrays (RA) are used in signal processing devices. Reflecting elements in the form of grooves fabricated by ion-plazma etching in a piezosubstrate are most widely used. In the geometry of such filters, input and output unidistant interdigital transducers IDT and U-path RA ca be used [1] (Fig. 1a).

Propagating from the input transducer to the output one, an acoustic wave reflects on 90 deg two times (on the upper and lower gratings). To reduce multireflections inside the grating, the grooves are fabricated with low depth ($i/\lambda = 0.03$, where h-groove depth, λ – SAW wavelength). The drawbacks of this geometry are a relatively narrow band (30%) and high ripples of amplitude-frequency and phase-frequency responses due to SAW multireflections in RA. Increasing of device bandwith leads to the growth of insertion losses.

RAC with dispersive IDT and slanted RA are known [2]. The example of this device is shown in Fig. 1(b). This geometry of IDT has space-frequency selectivity. When the frequency of the exciting harmonic signal sweeps f_l to f_h, the acoustic beam of

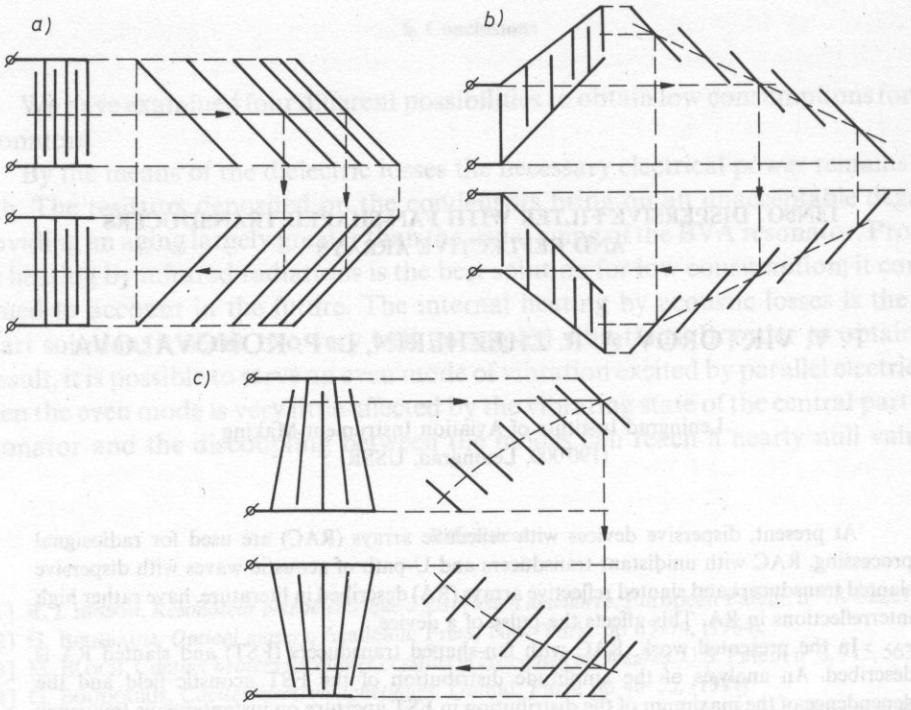

FIG. 1. Different RAC types

the slanted dispersive transducer shifts upwards in the transducer aperture. Beam width depends on the transducer's bandwith, aperture, and the angle of inclination of the transducer central line to the longitudinal axis of the device. The elements of RA are placed in a such way that in any longitudinal section it matches the condition

$$\Lambda_t = \Lambda_{RA},$$

where Λ_t is the distance between the adjacent fingers of IDT in an arbitrary section, Λ_{RA} the distance between the adjacent grooves in the same section. Space-frequency separation of reflecting channels reduces multireflections in RA. But the number of weak-dependent channels does not exceed 3–5. Also, in RAC slanted dispersive transducers and RA are used [3].

2. Analysis of FST acoustic field

In the designed dispersive filter, fan-shaped transducers FST and slanted RA are used. The geometry of the device is shown in Fig. 1(c). FST has high space-frequency selectivity [5]. Figure 2 shows the amplitude distribution, computed with a specially

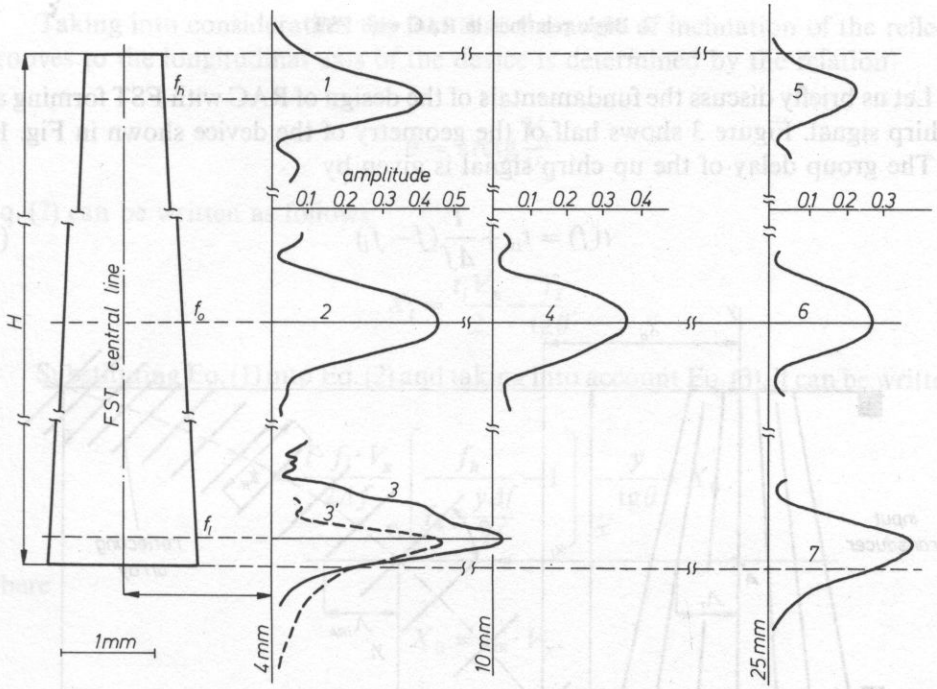

FIG. 2. Amplitude distribution of SAW FST acoustic field

written program, of the acoustic field in the aperture of FST at several distances from the longitudinal axis the distances are shown in brackets. The program accounts for SAW velocity anisotropy in the piezosubstrate (YZ-$LiNbO_3$). The field distribution on single frequency is characterized by the $\sin(x)/x$ function. The beam width can be estimated with a certain level of the function. The distribution (1) corresponds to high frequency of the exciting frequency band – f_h, 2 – to central frequency f_0, 3 – lower frequency f_l. The plots (1)–(5), (2)–(4)–(6) and (3)–(7) show changes in the distributions on the frequencies with the distance from the transducer's axis increasing. The relative bandwith of the transducer $\Delta f/f$ is 0.5 $f_h = 1.25\ f$, $f_l = 0.75\ f$. The fan's opening angle is 3 deg, the transducer aperture H is 7.7 mm. The plots show that in an aperture of FST, a great number actually 10–15 of weak-coupled acoustic channels can exist. Thus FST chances of being used to create RAC with reduced interreflections between RA elements are good.

However, as seen in Fig. 2 the drawbacks of the field structure are the decreased maximum value of the distribution function and broadening of the function. At great distances from the transducer's axis, the function can have be no explicit maximum on the frequency. In FST, the position of the acoustic beam in a device aperture depends on the frequency of an exciting harmonic signal hyperbolically [5]. That affects the RA geometry of the device.

3. Basic relations in RAC with FST

Let us briefly discuss the fundamentals of the design of RAC with FST forming an up chirp signal. Figure 3 shows half of the geometry of the device shown in Fig. 1c.

The group delay of the up chirp signal is given by

$$t(f) = t_{\text{in}} + \frac{T}{\Delta f}(f - f_l) \tag{1}$$

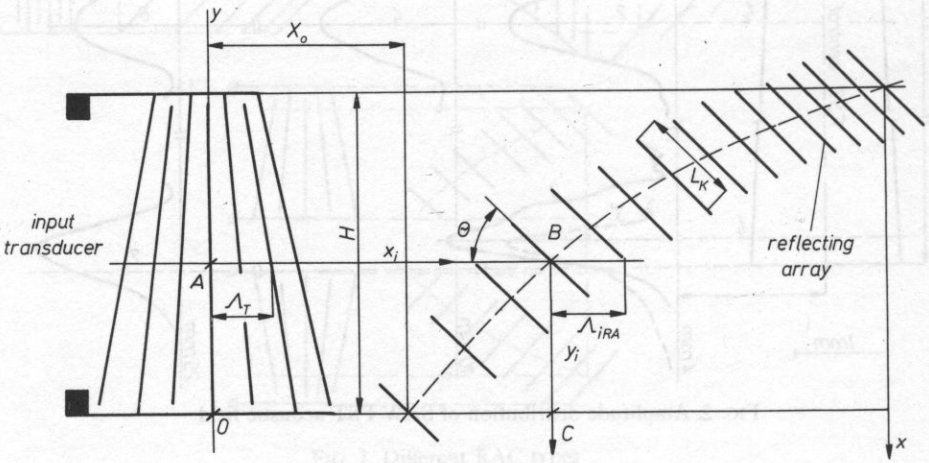

FIG 3. RAC-FST layout (one half represented)

where t_{in} – initial delay, T – signal duration, Δf – pulse frequency sweep, f_l – lower frequency.

In the coordinate system introduced in Fig. 3, any i-th delay is determined by the relation

$$\frac{t_i}{2} = \frac{AB}{V_x} + \frac{BC}{V_y} = \frac{X_i}{V_x} + \frac{Y_i}{V_y} \tag{2}$$

where V_x and V_y are the velocities in longitudinal and transverse directions.

For FST shown in Fig. 3 the following expressions is correct

$$f(y) = \frac{f_e}{1 - \dfrac{y\Delta f}{H f_h}} \tag{3}$$

where f_l and f_h – lower and upper edges of the transducer's operating band f – instantaneous frequency, y – coordinate of acoustic beam position, H – transducer's aperture.

Taking into consideration the fact that the angle of inclination of the reflecting grooves to the longitudinal axis of the device is determined by the relation

$$\theta = \operatorname{arctg} \frac{V_y}{V_x}. \tag{4}$$

Eq. (2) can be written as follows:

$$X_i = \frac{t_i V_x}{2} - \frac{Y_i}{\operatorname{tg}\theta}. \tag{5}$$

Substituting Eq. (1) into Eq. (2) and taking into account Eq. (3), it can be written as

$$x = \frac{T \cdot f_l \cdot V_x}{2\Delta f} \left(\frac{f_h}{f_h - \dfrac{y\Delta f}{H}} - 1 \right) - \frac{y}{\operatorname{tg}\theta} + X_0 \tag{6}$$

where

$$X_0 = t_{in} \cdot V_x.$$

The relation (6) describes the shape of the central line of reflecting grating. The length of the k-th groove is determined by the width of the acoustic beam in groove position (on the transducer's aperture and at a distance from the fan axis).

The total signal duration is formed by both gratings, as shown in Fig. 1(c).

The layout of a compressive filter is shown in Fig. 4. The expansive and compressive devices shown in Figs. 1(c) and 4 realize the maximum dispersion in the pulse being formed. The minimum delay in the filters shown in Figs. 4 and 5 is determined by the path of the beam propagating along the trajectory *1*, and the maximum delay by the path along the trajectory *2*.

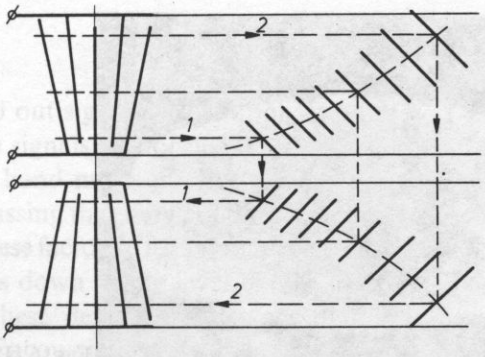

FIG. 4. Compression RAC with increased dispersion

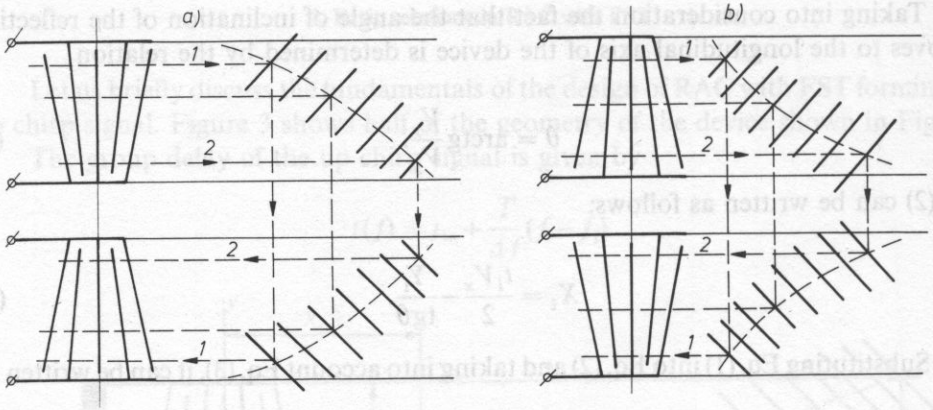

FIG. 5 a) Expansion RAC with decreased dispersion; b) Compression RAC with decreased dispersion

Dispersion in the signal being formed is the difference between these paths. Filters with the position of transducers and RA as shown in Fig. 5 realize the minimum pulse dispersion.

4. Experimental results

Dispersive devices with FST and slanted RA made on YZ-$LiNbO_3$ have been designed. The layouts of expansion and compression lines shown in Figs 1(c) and 4 have been used. In the compression line, RA has been apodized by changing the length of the reflective elements. Grooves with a constant relative depth $h/\lambda = 0.03$ are fabricated by ion-plasma etching. A radiopulse with duration $T = 16$ μs has been formed, the relative bandwith $\Delta f/f_0 = 40\%$. The pluse response of the expansion filter is shown in Fig. 6 (the scales 2 μs/div). Figure 7(a) shows the signal in the output of the compression filter the scales 50 ns/div. Figure 7(b) shows the same signal 20 times expanded vertically (the scales 25 ns/div). The estimated level of the side lobes is 28–30 dB.

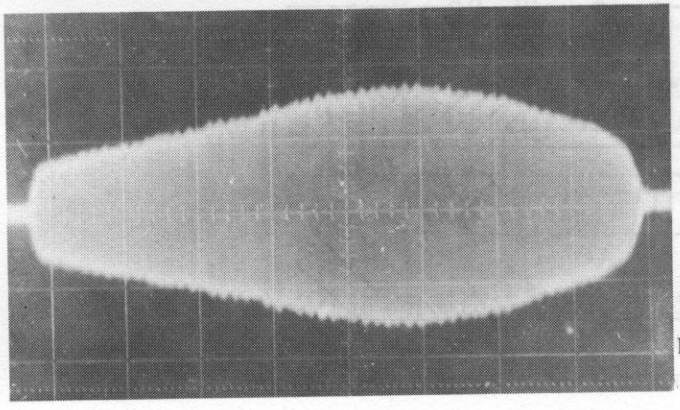

FIG. 6. Pulse response of the expansion filter. The scales: 2 μs/div.

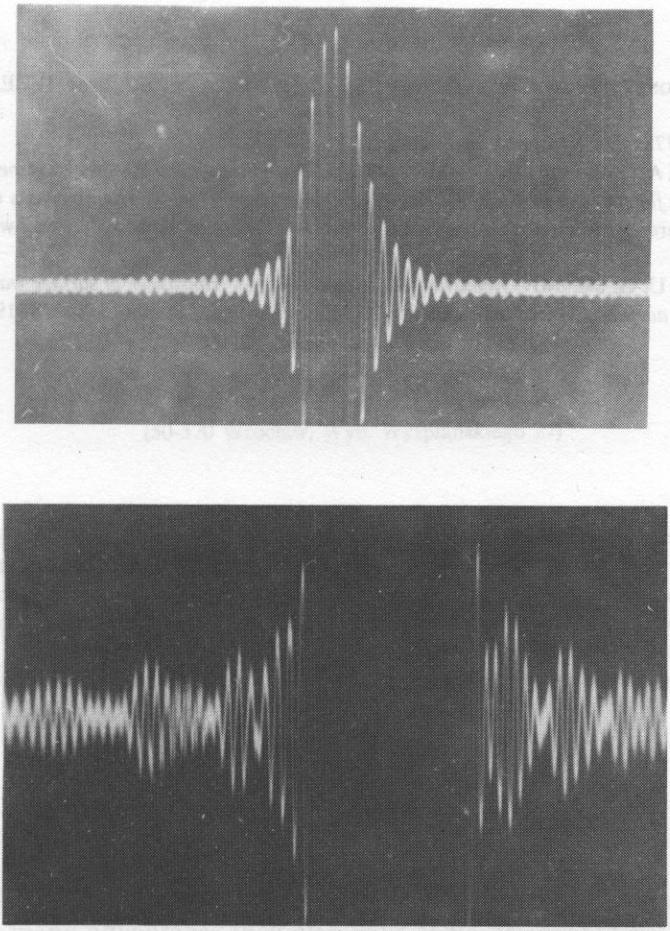

FIG. 7. a) Compressed signal in the output of the compression filter. The scales: 50 ns/div., 0.2 V/div.; b) Compressed signal in the output of the compression filter. The scales: 25 ns/div., 0.01 V/div.

The research carried out signals future application of FST in RAC. When wide-band (up to 100%) chirp signals are formed, FST transducers electric energy into an acoustic one in a whole band more effectively. FST increases the dynamic range of a device as a result of focussing the energy of the acoustic field into a narrow beam (Fig. 2). The combination of these factors with $LiNbO_3$ being used as a piezosubstrate allows to reduce insertion losses down to the level of (25–30 dB).

The drawback of these devices, is the fact that it is necessary to take into consideration changes of acoustic beam width along the distance from the fan's axis. This increases the drop of the pulse response of the "unweighed" device.

References

[1] R. C. WILLIAMSON, *Properties and applications of reflective-array devices*, Proc. IEEE, **64**, 5, 702–710 (1976).

[2] US Patent 4477784, SAW dispersive delay-line.

[3] P. V. VICTOROV, A. G. ZHEZHERIN, I. S. MITROFANOV, *Computation and design of a dispersive device with reflective arrays for forming and compression of wideband chirp signals.* The abstracts of the report on All-Union conference "Acoustoelectronic devices for information processing". Moscow, 379–380 (1988) (Russ).

[4] S. A. ZABUZOV, U. G. SMIRNOV, *Acoustic field of a fan-shaped transducer of surface waves. Radiosignal processing with acustoelectronic and acustooptic devices*, Nauka, Leningrad, 14–18 (1983) (Russ.).